

1

2 Category: Original Article (invited)

3

4 **State-space Modeling Clarifies Productivity Regime Shifts of Japanese**
5 **Flying Squid**

6

7 Shota Nishijima^{1,*}, Hiroshi Kubota², Toshiki Kaga¹, Suguru Okamoto¹, Hisae

8 Miyahara², and Hiroshi Okamura¹

9

10 1: National Research Institute of Fisheries Science, Japan Fisheries Research and

11 Education Agency, 2-12-4 Fukuura, Kanagawa-ku, Yokohama, Kanagawa 236-8648,

12 JAPAN

13 2: Japan Sea National Fisheries Research Institute, Japan Fisheries Research and

14 Education Agency, 1-5939-22, Suido-cho, Chuou-ku, Niigata, Niigata 951-8121,

15 JAPAN

16

17 *Corresponding author: Shota Nishijima

18 E-mail: nishijimash@gmail.com; nishijimash@affrc.go.jp

19

20

21 ABSTRACT (150-200 words)

22 Regime shifts of climatic and environmental conditions potentially affect productivity
23 of fisheries resources, posing challenging issues to stock management. The stocks of the
24 Japanese flying squid (*Todarodes pacificus*) are suspected to suffer from regime shifts,
25 but their detection is difficult and possibly doubtful because the nature of short-lived
26 species readily makes the effect of regime shifts confounded with observation errors.
27 Here we developed a new state-space assessment model to evaluate the influence of
28 regime shifts on spawner-recruitment relationship of the Japanese flying squid. The
29 model simultaneously estimates the population dynamics of multiple stocks that could
30 share some life history parameters, making parameter inference stable. We demonstrate
31 that two-time regime shifts of productivity around 1991 and 2015 caused two- to
32 three-fold changes of maximum sustainable yields. The model with regime shifts
33 clarifies the relationship between fishing pressure and spawner abundance that is difficult
34 to detect in a model with no regime shift. The state-space approach will be a promising
35 tool to accurately assess stock status by separating recruitment process from observation
36 errors and contribute to the management of marine biological resources sensitive to
37 regime shifts.

38

39 *Keywords (up to 5)*

40 Japanese common squid; MSY reference points; multistock modeling; state-space stock
41 assessment model (SAM) ; template model builder (TMB)

42

43 INTRODUCTION

44 Ecological regime shifts cause drastic changes of ecosystem states and organisms
45 (Scheffer et al. 2001; Kadowaki et al. 2018). In the ocean, climatic and environmental
46 conditions drive regime shifts in productivity of fisheries stocks: average recruitment
47 for a certain period is substantially different before and after a single year (Perälä and
48 Kuparinen 2015; Maunder and Thorson 2019). Recent studies showed that a high
49 proportion of stocks experienced shifts of recruitment, or nonstationary
50 stock-recruitment relationship (Vert-Pre et al. 2013; Perälä and Kuparinen 2015;
51 Szuwalski et al. 2015). Since fisheries production is one of the most important
52 provisioning ecosystem services, understanding regime-shift dynamics of fisheries
53 resources is a key issue toward the sustainable use of nature's contribution from marine
54 ecosystems.

55 Maximum sustainable yield (MSY) is an important concept for the assessment
56 and management of fish stocks around the world. International legal frameworks for
57 sustainable fisheries, the United Nations Convention on Law of the Seas (UNCLOS)
58 and the United Nations Fish Stocks Agreement (UNFSA), set an objective as the
59 maintenance and restoration of populations at stock biomass that produces MSY. The
60 Convention on Biological Diversity (CBD) and the Sustainable Development Goals
61 (SDGs) also outline the sustainable use and conservation of biological resources.
62 Although these international circumstances require the estimation of MSY worldwide
63 (Costello et al. 2012; Martell and Froese 2013; Punt et al. 2014; Ichinokawa et al. 2017),
64 the existence of regime shifts makes the calculation of MSY challenging, because
65 regime shifts are likely to generate multiple stock-recruitment relationships and thus
66 multiple MSY-based reference points. It is suggested that although management advice

67 should take into account recruitment variability by regime-shift-like behaviors (Vert-Pre
68 et al. 2013; King et al. 2015), regime-based harvest control rules (HCRs) generally have
69 high risk of overfishing when regimes are misidentified or regime shifts do not occur
70 (A'mar et al. 2009; Szuwalski and Punt 2013). Reliable assessment on the occurrence
71 and degree of regime shifts is needed for considering management strategies of fisheries
72 stocks exhibiting nonstationary recruitment.

73 The stocks of Japanese flying squid (*Todarodes pacificus*) are considered to
74 suffer from regime shifts in association with dynamic climatic conditions (Sakurai et al.
75 2002; Kidokoro et al. 2010; Kurota et al. 2020). Climatic shift in 1989 caused water
76 temperature warm and expanded spawning areas of this species in the Sea of Japan
77 (Sakurai et al. 2000; Kidokoro et al. 2010). Its paralarvae were likely to survive as a
78 result of warming temperature (Sakurai et al. 2000, 2013), and thus, the catch biomass
79 and abundance index rised dramatically since 1989 (Sakurai et al. 2002; Fig. 1). We
80 expect, therefore, that the effect of regime shift changed spawner-recruitment
81 relationship of this species. Furthermore, the opposite direction of shift might occur
82 recently because the catch biomass and abundance index have been decreasing (Fig. 1;
83 Kaga et al. 2019). Since the Japanese flying squid is preyed upon in great numbers by
84 large fish, such as mackerels (*Scomber japonicus* and *S. australasicus*) and bullfin tuna
85 (*Thunnus thynnus*), and marine mammals, such as dolphins (Sakurai et al. 2013), this
86 species has an important role in sustaining food webs in marine ecosystems. The
87 occurrence of regime shifts in this species is of serious concern to fishermen and
88 fisheries managers.

89 Distinguishing recruitment process and observation error is important for
90 accurately detecting regime shifts (King et al. 2015; Maunder and Thorson 2019).

91 Recently, the state-space stock assessment models (SAM) that estimate latent variables
92 such as abundance and fishing mortality as random effects have been developed and is
93 effective at separately estimating process and measurement errors (Nielsen and Berg
94 2014; Miller and Hyun 2017; Okamura et al. 2018). However, these models are
95 age-structured and not possible to apply to the Japanese flying squid, because its
96 life-span is a single year. Applying population dynamics modeling to the stock
97 assessment for a species with annual life-span is generally difficult, because one cannot
98 track the interannual depletion process of each cohort by fishing and natural death,
99 making parameter estimation unstable. In fact, annual stock assessment of the Japanese
100 flying squid has been conducted based on an abundance index and not used population
101 models (Kaga et al. 2019; Kubota et al. 2019). The stock assessment has therefore
102 confounded measurement and process errors and been likely to fluctuate unwantedly.
103 The calculation of MSY also increases the demand for state-space approach for the
104 Japanese flying squid, because the estimation error in recruitment should be directly
105 linked to the measurement error in spawner abundance (i.e., independent variable for
106 recruitment), which could be considered appropriately by using a state-space model
107 (Subbey et al. 2014; Brooks and Deroba 2015).

108 A possible solution to estimation difficulty and instability is joint modeling of
109 multispecies or multistocks rather than per-stock analysis (Thorson et al. 2013).
110 Dynamics of multiple species and stocks could be partially correlated if they share
111 environmental conditions (Thorson and Minto 2015; Thorson et al. 2016). The
112 assumption on a species having the same life history parameter between different stocks
113 could be valid and enable parsimonious and stably predictive modeling. Fortunately,
114 there are two different stocks of the Japanese flying squid (autumn-spawning stock and

115 winter-spawning stock) that have been independently assessed (Kaga et al. 2019;
116 Kubota et al. 2019), but may have correlated dynamics (Hoshino et al. 2014).

117 In this article, we developed a new model for multistocks of annual life-span
118 species, called ‘SAMUIKA’ (State-space Assessment Model Used for IKA (squid in
119 Japanese)), to investigate whether and how regime shifts occur in productivity of the
120 Japanese flying squid. We firstly performed intensive model selection by varying the
121 occurrence, parameter, year, and pattern of regime shifts. We then computed MSY-based
122 reference points from estimated spawner-recruitment relationship. Lastly, we evaluated
123 the past stock status relative to the MSY-based reference points.

124

125 MATERIAL AND METHODS

126 *Biology and fisheries of Japanese flying squid*

127 The Japanese flying squid is one out of the nine TAC (total allowable catch) species in
128 Japan, whose total catch are restrictly managed by output control, because it is
129 commercially important for Japanese fisheries (5% of total Japanese catch in 2014;
130 Kaga et al. 2017; Kubota et al. 2017). Japan has conducted annual stock assessments of
131 autumn-spawning stock and winter-spawning stock that have diferent distributions as
132 well as spawning seasons. The former stock is distributed in the Sea of Japan, whereas
133 the latter is mainly distributed in the Northwest Pacific near Japan when it migrates in
134 feeding season (Kidokoro et al. 2010). The Japanese flying squid is usually caught by
135 jigging in Japan, but other fisheries including bottom trawling, set net, and purse seine
136 also harvest the species especially for the winter-spawning stock (Kaga et al. 2019).

137

138 *State-space modeling*

139 Our state-space model SAMUIKA simultaneously describes the population dynamics of
140 autumn-spawning and winter-spawning stocks of Japanese flying squid, whose lifespan
141 is a single year. The squid individuals that survive from natural death and fishing after
142 recruitment become spawning adults:

$$S_{i,y} = N_{i,y} \times \exp(-F_{i,y} - M), \quad (1)$$

143 where $S_{i,y}$ is the number of spawning adults of stock i (A: autumn-spawning, W:
144 winter-spawning) in year y (this definition of subscripts will be applied hereafter), $N_{i,y}$ is
145 the number of recruits, or stock number. $F_{i,y}$ is the fishing mortality coefficient, while M
146 is the natural mortality coefficient and assumed to be 0.6, in accordance with the annual
147 stock assessment (Kaga et al. 2019; Kubota et al. 2019). The natural mortality
148 corresponded to a death rate during half-year fishing season (monthly mortality
149 coefficient was assumed to be 0.1). The interannual dynamics of fishing mortality
150 coefficient is described by a random walk, as with age-structured state-space assessment
151 model (Nielsen and Berg 2014):

$$\log F_{i,y} \sim \text{Normal}(\log F_{i,y-1}, \tau_i^2), \quad (2)$$

152 where τ_i^2 is the variance that controls the process error of random walk.

153 The number of recruits is expressed by the product of Beverton-Holt model and
154 process error:

$$N_{i,y} = \frac{a_{i,y} S_{i,y}}{1 + b_{i,y} S_{i,y}} \times \exp(\varepsilon_{i,y}), \quad (3)$$

155 where $a_{i,y}$ represents the number of recruits per spawning individual when adult number
156 approaches zero, and $b_{i,y}$ represents the strength of density dependence per spawning
157 individual. We consider that the spawner-recruitment parameters $a_{i,y}$ and $b_{i,y}$ could

158 depend not only stocks but also years because regime shifts could affect these
159 parameters (details are shown in the next subsection). $\varepsilon_{i,y}$ is a deviance to the
160 stock-recruitment curve and assumed to follow a multivariate normal distribution:

$$\varepsilon_y = (\varepsilon_{A,y}, \varepsilon_{W,y})' \sim \text{MVN}(\mathbf{0}, \Sigma_y). \quad (4)$$

161 Σ_y is a variance-covariance matrix:

$$\Sigma_y = \begin{pmatrix} \sigma_{A,y}^2 & \rho\sigma_{A,y}\sigma_{W,y} \\ \rho\sigma_{A,y}\sigma_{W,y} & \sigma_{W,y}^2 \end{pmatrix}, \quad (5)$$

162 where $\sigma_{i,y}^2$ is the variance in recruitment process and ρ is the correlation coefficient of
163 recruitment variability between two stocks. We used the multivariate normal distribution
164 because recruitment deviances could be correlated between autumn-spawning and
165 winter-spawning stocks that potentially share environmental and climatic conditions.
166 Moreover, we consider that the magnitude of recruitment variability could be different
167 between stocks and regimes.

168 The following observation model was fitted to data of catch biomass and
169 abundance index for autumn-spawning and winter-spawning stocks (Fig. 1; Kaga et al.
170 2019; Kubota et al. 2019). We used one time series of abundance index per stock that
171 was used in the annual stock assessment (Kaga et al. 2019; Kubota et al. 2019). The
172 duration of index data is 1981 to 2018 for the autumn-spawning stock and 1979 to 2017
173 for the winter-spawning stock (Table 1). The abundance indices were assumed to be
174 proportional to the stock numbers with normal errors at logarithmic scale:

$$\log I_{i,y} \sim \text{Normal}(\log(q_i N_{i,y}), \varphi_i^2), \quad (6)$$

175 where $I_{i,y}$ represents an index value, q_i represents a proportional constant, and φ_i^2 is the
176 variance that controls the magnitude of observation error. The observed catch biomass

177 was also followed to a normal distribution at logarithmic scale:

$$\log C_{i,y} \sim \text{Normal}(\log \hat{C}_{i,y}, \omega_i^2), \quad (7)$$

178 where $\hat{C}_{i,y}$ represents a predicted catch biomass and ω_i^2 is the variance in observation
179 error. The duration of catch data is 1979 to 2017 for both stocks (Table 1). We used the
180 Baranov equation to obtain the predicted catch biomass:

$$\hat{C}_{i,y} = w_{i,y} \times \frac{F_{i,y}}{F_{i,y} + M} \times N_{i,y} \times [1 - \exp(-F_{i,y} - M)], \quad (8)$$

181 where $w_{i,y}$ is mean body mass per individual. We used the body weight in the annual
182 stock assessment (Kaga et al. 2019; Kubota et al. 2019): for the autumn-spawning stock
183 the per-capita mass is 280g during the whole period, while for the winter-spawning
184 stock the per-capita mass is 300g before 1989 and 311g thereafter.

185

186 *Parameter estimation and model selection*

187 We estimated the parameters of fixed and random effects (Table 1) using the maximum
188 likelihood method via template model builder (TMB, Kristensen et al. 2016). TMB
189 enables the estimation of many random effects using the Laplace approximation and
190 automatic differentiation (Kristensen et al. 2016). Because the random effects were
191 estimated at the logarithmic scale, we applied a generic method for bias correction for
192 the mean of random effects (Thorson and Kristensen 2016). The source code and data
193 are made available as an R package at GitHub
194 (<https://github.com/ShotaNishijima/messir>).

195 TMB enables fast optimization of hierarchical models including complex
196 random effects (Kristensen et al. 2016). By utilizing this advantage, we analyzed a
197 number of models having different assumptions on recruitment and performed model

198 selection based on AICc (Burnham and Anderson 2002). We found that assuming that
199 both $a_{i,y}$ and $b_{i,y}$ were independent between stocks caused false convergence or
200 unrealistic, extremely-large abundance estimates, suggesting that estimation is
201 unfeasible only from one-stock information. We therefore assumed that at least either
202 $a_{i,y}$ or $b_{i,y}$ must be a common value between stocks. We also assumed that a regime shift
203 occurred simultaneously for both stocks and changed either $a_{i,y}$ or $b_{i,y}$ in the
204 spawner-recruitment relationship. This assumption was made because a previous study
205 suggested the shift in climatic conditions changed spawning areas and stock abundances
206 for both autumn-spawning and winter-spawning stocks (Sakurai et al. 2000). The
207 changes in $a_{i,y}$ and $b_{i,y}$ both caused the change in productivity, and therefore, were likely
208 to be confounded (Maunder and Thorson 2019). The variation in $a_{i,y}$ changes both
209 maximum recruits per spawner and maximum recruitment, and thus affects expected
210 recruitment at both high and low spawning abundances. On the other hand, the variation
211 in $b_{i,y}$ changes maximum recruitment, but not maximum recruits per spawner, and thus
212 affects expected recruitments at high spawning abundance.

213 To reduce the number of analyzed models, we assumed that the parameter that
214 are independent of stocks could change in response to a regime shift by considering that
215 the spawner-recruitment parameter that is different between stock is also likely to be
216 different among regimes; when the parameter $a_{i,y}$ (or $b_{i,y}$) was different between stocks,
217 $a_{i,y}$ (or $b_{i,y}$) could be different among regimes. When the same parameter values $a_{i,y}$ and
218 $b_{i,y}$ were shared between stocks, we assumed that either $a_{i,y}$ or $b_{i,y}$ changed due to a
219 regime shift. We thus made seven types of assumptions: (1) both parameters $a_{i,y}$ and $b_{i,y}$
220 were common between stocks and no regime shift occurred; (2) both parameters $a_{i,y}$ and
221 $b_{i,y}$ were common between stocks and a regime shift changed the parameter $a_{i,y}$; (3) both

222 paramters $a_{i,y}$ and $b_{i,y}$ were common between stocks and a regime shift changed the
223 parameter $b_{i,y}$; (4) the parameter $a_{i,y}$ were different between stocks ($b_{i,y}$ were common)
224 and no regime shift occurred; (5) the parameter $b_{i,y}$ were different between stocks ($a_{i,y}$
225 were common) and no regime shift occurred; (6) the parameter $a_{i,y}$ were different
226 between stocks ($b_{i,y}$ were common) and a regime shift changed the parameter $a_{i,y}$; and
227 (7) the parameter $b_{i,y}$ were different between stocks ($a_{i,y}$ were common) and a regime
228 shift changed the parameter $b_{i,y}$.

229 Previous studies suggests that a regime shift from low to high state occurred
230 around 1989 (Sakurai et al. 2002; Kidokoro et al. 2010), and another regime shift
231 possibly occurs in recent years (Kaga et al. 2019). We considered three patters of
232 regime shifts: (i) a regime shift occurred once in a year between 1987-1991 (A→B); (ii)
233 regime shifts occurred twice in a year between 1987-1991 and in a year between
234 2013-2017, respectively, and the second regime shift reverted the first state (A→B→A);
235 and (iii) regime shifts occurred twice in a year between 1987-1991 and in a year
236 between 2013-2017, respectively, and the second regime shift brought a third state
237 (A→B→C). The first patten had five cases having different shifting years, and the
238 second and third patterns had 25 cases (= 5×5), and thus we analyzed 55 cases
239 (5+15+25) in the models with regime shift(s). We had four out of the seven types that
240 assumed regime shift(s) in the previous paragraph (2, 3, 6 and 7). The other three types
241 with no regime shift had only one case respectively (1,4, and 5). We analyzed 223
242 models (= 55×4+3) with different assumptions in total.

243 We futher assumed the parameter τ_i^2 (variance representing process error of
244 fishing mortality coefficient) and ω_i^2 (variance representing observation error of catch)
245 were common between stocks (Table 1). This is because a preliminary analysis showed

246 that estimated values of these parameters varied little between stocks and assuming a
247 common value between stocks had lower AICc (Burnham and Anderson 2002) than
248 assuming different values in a preliminary analysis. We excluded 68 models that caused
249 estimation error or convergence problem from results; remaining 155 (223–68) models
250 achieved successful estimation and convergence. We calculated AICc of each of
251 successfully-converged models from maximum likelihood, sample size, and the number
252 of fixed parameters shown in Table 1.

253

254 *MSY-based reference points*

255 We calculated derived parameters and biological reference points from estimated
256 stock-recruitment relationships (Eq. 3). First, we obtained the steepness h , or the
257 fraction of recruitment from unfished population obtained when the spawning stock is
258 20% of its unfished level (Mangel et al. 2010):

$$hN_0 = \frac{a \times 0.2S_0}{1 + b \times 0.2S_0}. \quad (9)$$

259 N_0 and S_0 are the unfished numbers of recruits and spawners, respectively, which can be
260 obtained from the intersection of the spawner-recruitment relationship and the
261 replacement line ($y = \exp(M) \times x$ in this case):

$$S_0 = \frac{a - \exp(M)}{b \times \exp(M)} \text{ and } N_0 = \frac{a - \exp(M)}{b}. \quad (10)$$

262 $h = 1$ means that the recruitment is completely driven by environments, whereas $h = 0.2$
263 means the proportional relationship between spawners and recruits. The steepness,
264 therefore, represents the resilience of a species to harvesting: a high steepness indicated
265 high resilience, and vice versa (Mangel et al. 2010). In this study, we can calculate the

266 steepness by substituting the equation (10) into the equation (9):

$$h = \frac{a}{a + 4 \exp(M)}. \quad (10)$$

267 It is worth noting that the steepness depends on the parameter a but not b .

268 We then calculated MSY-based reference points. The amount of surplus
269 production reaches at maximum when the difference between spawner-recruitment
270 relationship and replacement line is the largest:

$$S_{MSY} = \frac{1}{b} \left\{ \sqrt{\frac{a}{\exp(M)}} - 1 \right\}, \quad (11)$$

$$N_{MSY} = \frac{aS_{MSY}}{1 + bS_{MSY}}, \quad (12)$$

271 and $F_{MSY} = \log(N_{MSY}) - \log(S_{MSY}) - M$. MSY was calculated by substituting N_{MSY} and F_{MSY}
272 into Eq. 8. We compared the estimates with these MSY-based reference points to
273 evaluate the stock status in the past. The steepness and MSY-based reference points
274 were computed for each parameter set of spawner-recruitment relationship when models
275 with different parameters between stocks and/or regimes were selected.

276

277 RESULTS

278 *Model selection*

279 Model selection showed that top models with lower AICc had two-time regime shifts
280 around 1991 and 2015 (Table 2). The models with one-time regime shift had $\Delta AICc$ of
281 21.7 or larger. The no-regime models had $\Delta AICc$ of 34.1 or larger, and were ranked as
282 the worst among the 155 models having successful convergence. For comparison, the
283 results of a no-regime model are shown in Supporting Information. The best five models

284 assumed different parameter values of the strength of density dependence ($b_{i,y}$) between
285 stocks and regimes, rather than the maximum number of recruits per spawning
286 individual ($a_{i,y}$). These five had different years of regime shifts, but the best model,
287 which assumed 1991 and 2015 as shifting years, had significantly lower ΔAICc than the
288 other models (ΔAICc of 4.2 or larger). The best three models assumed that the second
289 regime shift went back to the first regime ($A \rightarrow B \rightarrow A$), but the fourth model with ΔAICc
290 of 5.8 assumed different regimes between the first and third ones ($A \rightarrow B \rightarrow C$). The sixth
291 model with ΔAICc of 5.9 had different parameter values of the maximum number of
292 recruits per spawning individual ($a_{i,y}$), but a common value for the strength of density
293 dependence ($b_{i,y}$).

294

295 *Fit to observation*

296 The estimated temporal patterns of stock number were smoother than the temporal
297 dynamics of abundance indices especially for the autumn-spawning stock (Fig. 1b). The
298 stock number was kept at the low level during the first decade, and then abruptly
299 increased since the 1990s. This 'high' regime continued to a middle of the 2010s and
300 thereafter, the 'low' regime came back. The estimates of catch biomass were well fitted
301 to its observed values (Fig. 1a).

302

303 *Recruitment productivity*

304 The spawner-recruitment relationships were clearly distinct between the regimes in the
305 best model (Fig. 2). The Japanese flying squid belonged to the low regime in the 1980s,
306 and thereafter, moved to the high regime. The productivity then decreased to the low
307 regime in 2015. The magnitude of regime shift was larger for the winter-spawning

308 stock (Fig. 2b) than for the autumn-spawning stock (Fig. 2a). For the autumn-spawning
309 stock, the MSY in the high regime (305 thousand MT) was 1.8 times larger than that in
310 the low regime (167 thousand MT); for the winter-spawning stock, by contrast, the
311 MSY in the high regime (237 thousand MT) was 2.8 times larger than that in the low
312 regime (85 thousand MT) (Fig. 1a).

313 The spawner-recruitment relationship with regime shifts was considerably
314 different from that with no regime shift. The spawner-recruitment relationship became
315 close to a proportional relationship when we ignored regime shifts (Fig. S2 in
316 Supporting Information). The steepness was 0.83 in the best model with regime shifts,
317 but 0.35 in the model with no regime. This indicates that incorporating regime shifts
318 made the Japanese flying squid more resilient to harvesting.

319 Recruitment variability was higher in the winter-spawning stock than in the
320 autumn-spawning stock (Fig. 2). The recruitment variability was moderately correlated
321 between the stocks ($\rho = 0.69$).

322

323 *Fishing impact on spawners*

324 The temporal patterns of fishing mortality greatly differed between stocks. For the
325 autumn-spawning stock, the fishing mortality coefficient was higher than F_{MSY} in the
326 1980s, but gradually decreased to a much lower level than F_{MSY} (Fig. 3a). As a result ,
327 the spawning number of autumn-spawning stock was kept at a higher level than S_{MSY}
328 (Fig. 3b). The relationship between the relative fishing mortality coefficient (F/F_{MSY})
329 and the relative spawning abundance (S/S_{MSY}) showed a clear negative association (Fig.
330 4).

331 For the winter-spawning stock, the fishing mortality coefficient wandered

332 around the level of F_{MSY} (Fig. 3a). The fishing pressure was lower than F_{MSY} up to 1993,
333 but became higher from 1994 to 2001. Thereafter, although the fishing impact was kept
334 at a lower level than F_{MSY} up to 2013, it became higher again in recent years. The
335 spawning number thus stayed around the MSY level (S_{MSY}) (Fig. 3b). The relative
336 spawning abundance (S/S_{MSY}) exhibited an opposite trend of the relative fishing
337 mortality coefficient (F/F_{MSY}) (Fig. 4).

338 It is noteworthy that F_{MSY} was constant between regimes and between stocks
339 (Fig. 3a). This is because model selection favored the best model that shared the
340 maximum number of recruits per individuals ($a_{i,y}$), rather than the strength of density
341 dependence ($b_{i,y}$), and F_{MSY} depended only on $a_{i,y}$.

342 The patterns of fishing pressure and spawner abundance were substantially
343 different depending on whether we considered regime shifts or not, especially for the
344 winter-spawning stock. If we had ignored regime shifts, the fishing mortality would
345 have exceeded F_{MSY} (i.e., overfishing) and the spawning abundance would have been
346 lower than S_{MSY} (overfished) for the whole period of the winter-spawning stock (Fig. S3
347 in Supporting Information). The relationship between the relative fishing mortality
348 coefficient (F/F_{MSY}) and the relative spawning abundance (S/S_{MSY}) was unclear in the
349 model without regime (Fig. S4 in Supporting Information).

350

351 DISCUSSION

352 The state-space assessment model clarified that productivity regime shifts of the
353 Japanese flying squid occurred twice during the analyzed period. Previous studies based
354 on field surveys showed that the climatic shift from cool to warm condition caused the
355 expansion of spawning areas of this species around 1989 (Sakurai et al. 2000, 2013;

356 Kidokoro et al. 2010). The current study provides another line of supportive evidence of
357 regime shift for the Japanese flying squid, using population dynamics modeling.
358 Although the climatic shift was recognized to occur in 1989 (Yasunaka and Hanawa
359 2002), our results showed that the top model had the shifting year of 1991 (Table 2).
360 This might suggest a time lag of biological response of productivity to the climatic
361 effect or be a statistical artifact because the second top model selected 1989 as the
362 shifting year. The top models suggested that the second regime shift occurred around
363 2015 and the current state was identical to that in the 1980s, longer time-series data
364 would be needed to decide whether the current regime is truly the same as the 1980s.
365 Top models favored different parameter values of the strength of density dependence,
366 rather than maximum recruits per capita spawner, between regimes (Table 2). Combined
367 with biological studies showing that the survival rate of paralarvae varied in response to
368 climatic regimes (Sakurai et al. 2000, 2013), climate-driven regime shifts may affect a
369 density-dependent survival of paralarvae. Because TMB enables much faster parameter
370 inference than Bayesian MCMC algorithm, it is now easier than ever to analyze a
371 number of hierarchical models and perform intensive model selection like this study.
372 Random-effect models will be increasingly applied to various kinds of stock assessment
373 modeling (Thorson and Minto 2015).

374 SAMUIKA is a novel state-space stock assessment model in terms of
375 multistock modeling of annual life-span species. To check estimability, we conducted a
376 simple simulation test as an additional analysis by generating bootstrap data from
377 estimated models (Supporting Information). Results showed that the best model with
378 the lowest AICc could obtain almost unbiased estimates in abundances and fishing
379 mortalities (Fig. S5 in Supporting Information). However, the no-regime model

380 obtained seriously-biased estimates: overestimation of abundances and underestimation
381 of fishing mortalities (Fig. S6 in Supporting Information). This bias was caused because
382 the no-regime model had larger estimation uncertainty than the regime-shift model and
383 ignoring regime shifts was likely to mask fishing impacts (see Supporting Information
384 for details). Indeed, the regime-shift model estimated lower abundances and higher
385 fishing mortality coefficients than the no-regime model, suggesting that the regime-shift
386 model possibly obtained estimates closer to true values. Incorporating productivity
387 regime shifts into the assessment of the Japanese flying squid fundamentally important
388 for accurately estimating stock status.

389 Our concern on the model results is that estimation uncertainty in spawner
390 abundance was larger than that in recruitment (stock) abundance: average coefficient of
391 variation was 0.18 for stock numbers but 0.55 for spawning numbers. This is because
392 the used abundance indices were of recruitment abundance, but not spawner abundance.
393 The large uncertainty in spawner abundance may be problematic, because spawner
394 abundance is usually employed to judge stock status and its uncertainty is directly
395 linked to the reliability of stock assessment. Developing an abundance index for
396 spawners is an important future task toward more robust estimation.

397 Regime shifts caused twofold and threefold changes of MSY to the
398 autumn-spawning stock and the winter-spawning stock, respectively (Fig. 1). A reason
399 for the larger difference of MSY of the winter-spawning stock is that it migrates in large
400 areas off east coast of Japan in the Northwest Pacific including high seas, where the
401 Kuroshio and Oyashio Currents cause enormous decadal variation of environmental
402 factors (Yatsu et al. 2013). Compared to small pelagic fishes, however, the magnitude of
403 regime shifts is smaller for the stocks of the Japanese flying squid; for example, the

404 Pacific stock of the Japanese sardine (*Sardinops melanostictus*) has a 13-fold difference
405 of MSY between regimes (S. Furuichi, personal communication). We recognize,
406 therefore, that the Japanese flying squid probably exhibits the regime shift of
407 productivity, but its intensity is not so large.

408 Two major differences between the results with and without regime shifts can
409 be seen in the relationship between fishing mortality coefficient and spawner abundance
410 relative to the MSY-based reference points (Fig. 4 vs. Fig. S4 in Supporting
411 Information). First, the model with regime shifts showed a clearer negative correlation
412 between the relative fishing mortality. This suggests that ignoring regime shifts is likely
413 to obscure the impact of fishing and incorporating environmentally-driven productivity
414 shifts can greatly change our view of fishing influences on stock status. Second, the
415 stock status is more likely to be overfishing and overfished in the model with no regime
416 shift than in the model with regime shifts. This is because the no-regime model
417 presumed that the variation of recruitment was caused by the variation of spawner
418 abundance, rather than regime shifts, causing lower steepness and resilience to fishing
419 (Fig. 2 vs. Fig. S2 in Supporting Information). Accordingly, one may wrongly declare
420 overfishing and/or overfished of a stock, if one ignores truly-occurring regime shifts. A
421 similar result is obtained from a previous simulation study testing the effectiveness of
422 regime-based HCRs (Szuwalski and Punt 2013).

423 Although our model has demonstrated the occurrence of regime shifts for the
424 squid stocks, whether we should choose a regime-based HCR still remains uncertain.
425 Previous studies presented two risky situations of overfishing (Szuwalski and Punt
426 2013; King et al. 2015): (1) one wrongly applies a HCR for high regime when one
427 overlooks shifting from high to low regime; and (2) one wrongly applies a regime-based

428 HCR when regime shifts do not occur actually. These risks may not be high for the
429 stocks of Japanese flying squid, however. Our estimated F_{MSY} are common between the
430 high and low regimes (Fig. 3), and setting the F_{MSY} as a limit reference point will
431 possibly avoid overfishing even if one overlooks a high-to-low regime shift. In addition,
432 the estimates of stock abundance in the regime-shift model were smaller than those in
433 the no-regime model and, therefore, the estimated MSY in the high regime was not
434 larger than that in the no-regime model for the winter-spawning stock, although this was
435 not the case for the autumn-spawning stock (Fig. 1 vs. Fig. S1 in Supporting
436 Information). The risk of overfishing may thus be sufficiently low even if applying
437 regime-based HCRs to this species. On the other hand, we also expect that there is no
438 sufficient profit (i.e., increased catch) of using regime-based HCRs, because the
439 magnitude of regime shifts is not large. Management strategy evaluation (MSE) will be
440 useful to make a judgement on this indecisive debate. The state-space model can assist
441 the MSE as not only assessment model but also operating model.

442 Our state-space modeling highlights a future direction of fisheries stock
443 assessments. Currently, stock-recruitment relationships have sometimes been estimated
444 by ex-post analyses using the estimates in stock assessment as fixed like observed data
445 to detect nonstationary dynamics (Vert-Pre et al. 2013; Szuwalski et al. 2015; Kurota et
446 al. 2020). However, abundance estimates could vary depending on whether regime
447 shifts are incorporated into assessment models, as demonstrated by this study, and it is
448 ideal to estimate a stock-recruitment relationship within stock assessment models
449 (Subbey et al. 2014; Brooks and Deroba 2015). The state-space approach can be
450 extended by two ways. First is to incorporate environmental effects on recruitment
451 productivity, which can be alternative to regime-shift models and has a potential to

452 improve the ability of future projection of stock dynamics (King et al. 2015; Maunder
453 and Thorson 2019). Second, joint modeling of multispecies will be feasible by inferring
454 interspecific correlation in population dynamics. Although a multispecies
455 spatio-temporal model has recently been developed (Thorson 2019), multispecies
456 state-space assessment models are still rare (Thorson and Minto 2015), but will be
457 informative for evaluating and mechanistically understanding fish communities. These
458 two ways correspond to ecosystem- and community-based approaches. Such approaches
459 will play an important role in evaluating provisioning ecosystem services from fisheries
460 production as a whole, because single-species assessment is inefficient and may be
461 insufficient for whole-scale evaluation of ecosystem services. Integrating multispecies
462 and environmental effects into state-space assessment models will contribute to the
463 understanding of community dynamics and the sustainable use of marine ecosystem
464 services.

465

466 ACKNOWLEDGEMENTS

467 This study was funded by JSPS KAKENHI Grant Number 19K15905. This study was
468 partially supported by grants for marine fisheries stock assessment and evaluation in
469 Japanese waters from the Fisheries Agency and the Fisheries Research and Education
470 Agency of Japan.

471

472 REFERENCES

473 A'mar ZT, Punt AE, Dorn MW (2009) The impact of regime shifts on the performance
474 of management strategies for the Gulf of Alaska walleye pollock (*Theragra*
475 *chalcogramma*) fishery. Can J Fish Aquat Sci 66:2222–2242.

- 476 <https://doi.org/10.1139/F09-142>
- 477 Brooks EN, Deroba JJ (2015) When “data” are not data: The pitfalls of post hoc
478 analyses that use stock assessment model output. *Can J Fish Aquat Sci* 72:634–641.
479 <https://doi.org/10.1139/cjfas-2014-0231>
- 480 Burnham KP, Anderson DR (2002) Model selection and multimodel inference. In: A
481 Practical Information-Theoretic Approach, 2nd ed. Springer-Verlag, New York,
482 USA, pp 49–97
- 483 Costello C, Ovando D, Hilborn R, et al (2012) Status and solutions for the world’s
484 unassessed fisheries. *Science* (80-) 338:517–521
- 485 Hoshino E, Milner-Gulland EJ, Hillary RM (2014) Why model assumptions matter for
486 natural resource management: Interactions between model structure and life
487 histories in fishery models. *J Appl Ecol* 51:632–641.
488 <https://doi.org/10.1111/1365-2664.12225>
- 489 Ichinokawa M, Okamura H, Kurota H (2017) The status of Japanese fisheries relative to
490 fisheries around the world. *ICES J Mar Sci* 74:1277–1287.
491 <https://doi.org/10.1093/icesjms/fsx002>
- 492 Kadowaki K, Nishijima S, Kéfi S, et al (2018) Merging community assembly into the
493 regime-shift approach for informing ecological restoration. *Ecol Indic* 85:991–998.
494 <https://doi.org/10.1016/j.ecolind.2017.11.035>
- 495 Kaga T, Yamashita N, Okamoto S, Funamoto T (2017) Stock assessment and evaluation
496 for the autumn-spawning stock of Japanese flying squid (fiscal year 2016). In:
497 Marine fisheries stock assessment and evaluation for Japanese waters (fiscal year
498 2016/2017). Fisheries Agency and Fisheries Research and Education Agency of

- 499 Japan., pp 618–657
- 500 Kaga T, Yamashita N, Okamoto S, Hamatsu Y (2019) Stock assessment and evaluation
501 for the winter-spawning stock of Japanese flying squid (fiscal year 2018). In:
502 Marine Fisheries Stock Assessment and Evaluation for Japanese Waters (fiscal
503 year 2018/2019). Fisheries Research and Education Agency of Japan, pp 652–697
- 504 Kidokoro H, Goto T, Nagasawa T, et al (2010) Impact of a climate regime shift on the
505 migration of Japanese common squid (*Todarodes pacificus*) in the Sea of Japan.
506 ICES J Mar Sci 67:1314–1322. <https://doi.org/10.1093/icesjms/fsq043>
- 507 King JR, McFarlane GA, Punt AE (2015) Shifts in fisheries management: adapting to
508 regime shifts. *Philos Trans R Soc B Biol Sci* 370:20130277.
509 <https://doi.org/10.1098/rstb.2013.0277>
- 510 Kristensen K, Nielsen A, Berg CW, et al (2016) TMB: Automatic differentiation and
511 laplace approximation. *J Stat Softw* 70:1–21. <https://doi.org/10.18637/jss.v070.i05>
- 512 Kubota H, Goto T, Miyahara H, Matsukura R (2017) Stock assessment and evaluation
513 for Japanese flying squid (fiscal year 2016). In: Marine fisheries stock assessment
514 and evaluation for Japanese waters (fiscal year 2016/2017). Fisheries Research and
515 Education Agency of Japan, pp 658–693
- 516 Kubota H, Miyahara H, Matsukura R (2019) Stock assessment and evaluation for the
517 autumn-spawning stock of Japanese flying squid (fiscal year 2018). In: Marine
518 Fisheries Stock Assessment and Evaluation for Japanese Waters (fiscal year
519 2018/2019). Fisheries Research and Education Agency of Japan, pp 698–745
- 520 Kurota H, Szuwalski CS, Ichinokawa M (2020) Drivers of recruitment dynamics in
521 Japanese major fisheries resources: Effects of environmental conditions and

- 522 spawner abundance. *Fish Res* 221:105353.
523 <https://doi.org/10.1016/j.fishres.2019.105353>
- 524 Mangel M, Brodziak J, DiNardo G (2010) Reproductive ecology and scientific
525 inference of steepness: A fundamental metric of population dynamics and strategic
526 fisheries management. *Fish Fish* 11:89–104.
527 <https://doi.org/10.1111/j.1467-2979.2009.00345.x>
- 528 Martell S, Froese R (2013) A simple method for estimating MSY from catch and
529 resilience. *Fish Fish* 14:504–514.
530 <https://doi.org/10.1111/j.1467-2979.2012.00485.x>
- 531 Maunder MN, Thorson JT (2019) Modeling temporal variation in recruitment in
532 fisheries stock assessment: A review of theory and practice. *Fish Res* 217:71–86.
533 <https://doi.org/10.1016/j.fishres.2018.12.014>
- 534 Miller TJ, Hyun S-Y (2017) Evaluating evidence for alternative natural mortality and
535 process error assumptions using a state-space, age-structured assessment model.
536 *Can J Fish Aquat Sci* cjfas-2017-0035. <https://doi.org/10.1139/cjfas-2017-0035>
- 537 Nielsen A, Berg CW (2014) Estimation of time-varying selectivity in stock assessments
538 using state-space models. *Fish Res* 158:96–101.
539 <https://doi.org/10.1016/j.fishres.2014.01.014>
- 540 Okamura H, Yamashita Y, Ichinokawa M, Nishijima S (2018) Comparison of the
541 performance of age-structured models with few survey indices. *ICES J Mar Sci*
542 fsy126. <https://doi.org/https://doi.org/10.1093/icesjms/fsy126>
- 543 Perälä T, Kuparinen A (2015) Detecting regime shifts in fish stock dynamics. *Can J*
544 *Fish Aquat Sci* 72:1619–1628. <https://doi.org/10.1139/cjfas-2014-0406>

- 545 Punt AE, Smith ADM, Smith DC, et al (2014) Selecting relative abundance proxies for
546 BMSY and BMEY. *ICES J Mar Sci* 71:469–483.
547 <https://doi.org/10.1093/icesjms/fst162>
- 548 Sakurai Y, Kidokoro H, Yamashita N, et al (2013) *Todarodes pacificus*, Japanese
549 common squid. Nova Science Publishers, Inc., New York, USA
- 550 Sakurai Y, Kiyofuji H, Saitoh S, et al (2000) Changes in inferred spawning areas of
551 *Todarodes pacificus* (Cephalopoda: Ommastrephidae) due to changing
552 environmental conditions. *ICES J Mar Sci* 57:24–30.
553 <https://doi.org/10.1006/jmsc.2000.0667>
- 554 Sakurai Y, Kiyofuji H, Saitoh S, et al (2002) Stock fluctuations of the Japanese
555 common squid, *Todarodes pacificus*, related to recent climate changes. *Fish Sci*
556 68:226–229. https://doi.org/10.2331/fishsci.68.sup1_226
- 557 Scheffer M, Carpenter S, Foley JA, et al (2001) Catastrophic shifts in ecosystems.
558 *Nature* 413:591–6. <https://doi.org/10.1038/35098000>
- 559 Subbey S, Devine JA, Schaarschmidt U, Nash RDM (2014) Modelling and forecasting
560 stock-recruitment: Current and future perspectives. *ICES J Mar Sci* 71:2307–2322.
561 <https://doi.org/10.1093/icesjms/fsu148>
- 562 Szuwalski CS, Punt AE (2013) Fisheries management for regime-based ecosystems: A
563 management strategy evaluation for the snow crab fishery in the eastern Bering Sea.
564 *ICES J Mar Sci* 70:955–967. <https://doi.org/10.1093/icesjms/fss182>
- 565 Szuwalski CS, Vert-Pre KA, Punt AE, et al (2015) Examining common assumptions
566 about recruitment: a meta-analysis of recruitment dynamics for worldwide marine
567 fisheries. *Fish Fish* 16:633–648. <https://doi.org/10.1111/faf.12083>

- 568 Thorson JT (2019) Guidance for decisions using the Vector Autoregressive
569 Spatio-Temporal (VAST) package in stock, ecosystem, habitat and climate
570 assessments. *Fish Res* 210:143–161. <https://doi.org/10.1016/j.fishres.2018.10.013>
- 571 Thorson JT, Ianelli JN, Larsen EA, et al (2016) Joint dynamic species distribution
572 models: a tool for community ordination and spatio-temporal monitoring. *Glob*
573 *Ecol Biogeogr* 25:1144–1158. <https://doi.org/10.1111/geb.12464>
- 574 Thorson JT, Kristensen K (2016) Implementing a generic method for bias correction in
575 statistical models using random effects, with spatial and population dynamics
576 examples. *Fish Res* 175:66–74. <https://doi.org/10.1016/j.fishres.2015.11.016>
- 577 Thorson JT, Minto C (2015) Mixed effects: a unifying framework for statistical
578 modelling in fisheries biology. *ICES J Mar Sci* 72:1245–1256.
579 <https://doi.org/10.1093/icesjms/fsu213>
- 580 Thorson JT, Stewart IJ, Taylor IG, Punt AE (2013) Using a recruitment-linked
581 multispecies stock assessment model to estimate common trends in recruitment for
582 US West Coast groundfishes. *Mar Ecol Prog Ser* 483:245–256.
583 <https://doi.org/10.3354/meps10295>
- 584 Vert-Pre KA, Amoroso RO, Jensen OP, Hilborn R (2013) Frequency and intensity of
585 productivity regime shifts in marine fish stocks. *Proc Natl Acad Sci U S A*
586 110:1779–1784. <https://doi.org/10.1073/pnas.1214879110>
- 587 Yasunaka S, Hanawa K (2002) Regime shifts found in the Northern Hemisphere SST
588 field. *J Meteorol Soc Japan* 80:119–135. <https://doi.org/10.2151/jmsj.80.119>
- 589 Yatsu A, Chiba S, Yamanaka Y, et al (2013) Climate forcing and the Kuroshio/Oyashio
590 ecosystem. *ICES J Mar Sci* 70:922–933. <https://doi.org/10.1093/icesjms/fst084>

591

592

593

594 TABLES

595 Table 1: List of symbols with their definitions, types, and constraint

Symbol	Definition	Type ¹	Constraint
$I_{i,y}$	Abundance index (1981-2018 for autumn-spawning stock, 1979-2017 for winter-spawning stock)	Data	-
$C_{i,y}$	Catch biomass (1979-2017 for both stocks)	Data	-
$w_{i,y}$	Per-capita body mass (1979-2017 for both stocks)	Data	-
M	Natural mortality coefficient	Assumed	0.6
τ_i	Standard deviation of process error in random walk of fishing mortality coefficient	Fixed	Common between stocks
$a_{i,y}$	Maximum number of recruits per spawning individual	Fixed	At least either $a_{i,y}$ or $b_{i,y}$ is common between stocks and regimes
$b_{i,y}$	Strength of density dependence per spawning individual	Fixed	
$\sigma_{i,y}$	Standard deviation of recruitment variability	Fixed	-
ρ	Correlation coefficient of recruitment variability between stocks	Fixed	-
$q_{i,j}$	Proportional constant for abundance index	Fixed	-
ϕ_i	Standard deviation of observation error for abundance index	Fixed	-
ω_i	Standard deviation of observation error for catch biomass	Fixed	Common between stocks
$F_{i,y}$	Fishing mortality coefficient	Random	-
$N_{i,y}$	Number of recruits (stock number)	Random	-
$S_{i,y}$	Number of spawning adults	Derived	-
$\varepsilon_{i,y}$	Recruitment deviation to stock-recruitment relationship	Derived	-
i	Stock (A: autumn-spawning, W: winter-spawning)	Subscript	-

y	Fishing year	Subscript	-
---	--------------	-----------	---

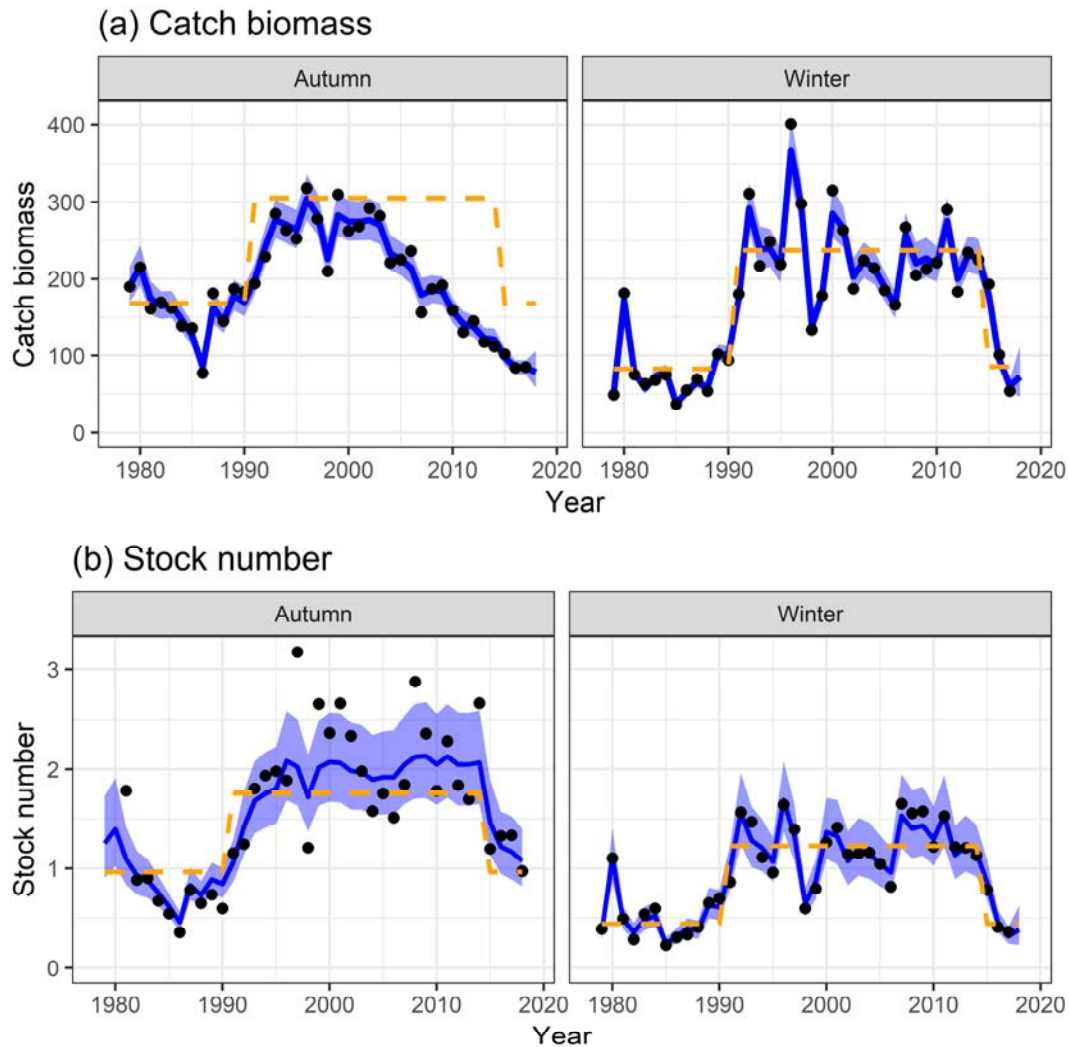
596 1: "Fixed", "Random", and "Derived" are the types of parameters.

597 Table 2: Model selection table for top ten models, the best model with one-time regime-shift, and the best model with no regime

Rank	AICc	Δ AICc	Log-likelihood	Number of parameters	Regime pattern	Shifting year	Per-regime parameter	Per-stock parameter
1	18.12	0.00	8.91	16	A → B → A	1991 & 2015	<i>b</i>	<i>b</i>
2	22.37	4.25	6.79	16	A → B → A	1989 & 2015	<i>b</i>	<i>b</i>
3	23.26	5.14	6.34	16	A → B → A	1990 & 2015	<i>b</i>	<i>b</i>
4	23.93	5.81	11.17	20	A → B → C	1991 & 2016	<i>b</i>	<i>b</i>
5	23.98	5.86	5.98	16	A → B → A	1989 & 2016	<i>b</i>	<i>b</i>
6	24.01	5.89	5.96	16	A → B → A	1989 & 2015	<i>a</i>	<i>a</i>
7	24.28	6.16	5.83	16	A → B → A	1991 & 2014	<i>b</i>	<i>b</i>
8	24.78	6.66	5.58	16	A → B → A	1990 & 2016	<i>b</i>	<i>b</i>
9	25.04	6.92	10.61	20	A → B → C	1991 & 2015	<i>b</i>	<i>b</i>
10	25.27	7.15	5.33	16	A → B → A	1991 & 2014	<i>a</i>	<i>a</i>
...
101	39.80	21.68	-1.93	16	A → B	1989	<i>b</i>	<i>b</i>
153	52.22	34.10	-13.01	12	A	-	-	<i>a</i>

599 FIGURES

600 *Figure 1:*



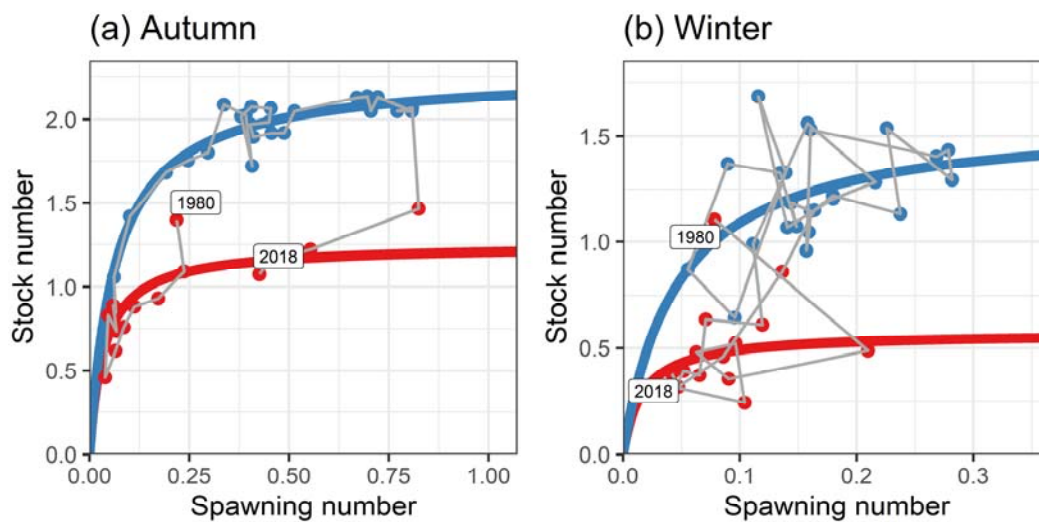
601

602 Time series of (a) catch biomass (thousand MT) and (b) stock number (billion) for the
603 autumn-spawning stock (left) and the winter-spawning stock (right). The black points
604 indicate (a) observed catch biomass and (b) abundance index divided by the
605 proportional constant (I_i/q_i). The blue solid lines and shadowed areas indicate point
606 estimates and their 80% confidence intervals, respectively. The orange dashed lines
607 indicate (a) MSY and (b) the stock number at the MSY-level equilibrium (N_{MSY}).

608

609

610 *Figure 2:*



611

612 Spawner-recruitment relationships of (a) the autumn-spawning stock and (b) the

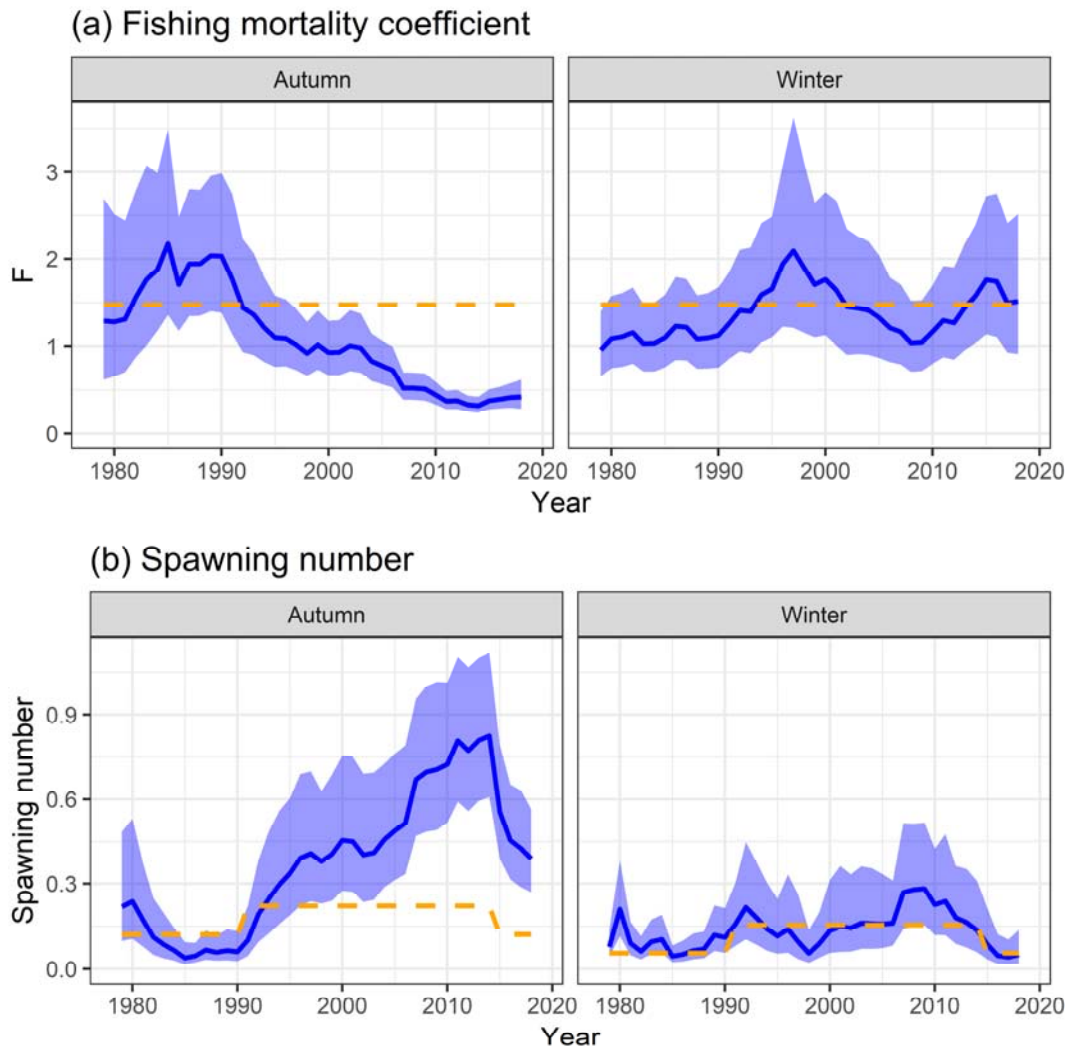
613 winter-spawning stock. The red and blue lines indicates the low and high regimes,

614 respectively.

615

616

617 Figure 3:



618

619 Time series of (a) fishing mortality coefficient and (b) spawning number (billion)

620 for the autumn-spawning stock (left) and the winter-spawning stock (right). The blue

621 solid lines and shadowed areas indicate point estimates and their 80% confidence

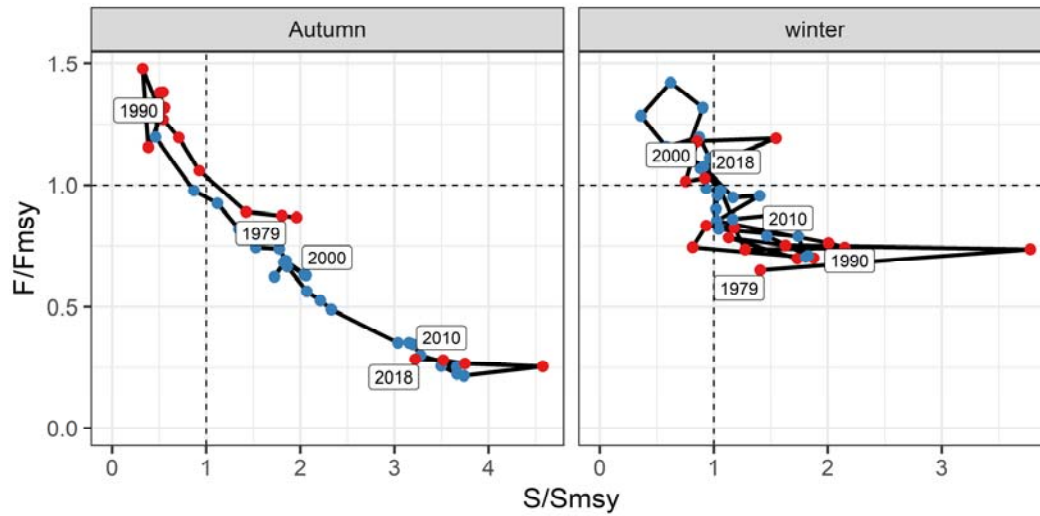
622 intervals, respectively. The orange dashed lines indicate the MSY-level equilibrium

623 (F_{MSY} and S_{MSY}).

624

625

626 *Figure 4:*



627

628 Relationships between fishing mortality coefficient and spawner abundance relative to
629 the MSY-based reference points for the autumn-spawning stock (left) and the
630 winter-spawning stock (right). The red and blue lines indicates the low- and
631 high-regimes, respectively.

632